AVS JVSTB Journal of Vacuum Science & Technology B

Morphology control of silicon nanotips fabricated by electron cyclotron resonance plasma etching

C. H. Hsu, Y. F. Huang, L. C. Chen, S. Chattopadhyay, K. H. Chen, H. C. Lo, and C. F. Chen

Citation: Journal of Vacuum Science & Technology B **24**, 308 (2006); doi: 10.1116/1.2163894
View online: http://dx.doi.org/10.1116/1.2163894
View Table of Contents: http://scitation.aip.org/content/avs/journal/jvstb/24/1?ver=pdfcov
Published by the AVS: Science & Technology of Materials, Interfaces, and Processing

Articles you may be interested in

Silicon nitride nanotemplate fabrication using inductively coupled plasma etching process
J. Vac. Sci. Technol. B **29**, 051802 (2011); 10.1116/1.3628593

Trap density of GeNx/Ge interface fabricated by electron-cyclotron-resonance plasma nitridation
Appl. Phys. Lett. **99**, 022902 (2011); 10.1063/1.3611581

Self-organized vertically aligned single-crystal silicon nanostructures with controlled shape and aspect ratio by reactive plasma etching
Appl. Phys. Lett. **95**, 111505 (2009); 10.1063/1.3232210

In vacuo substrate pretreatments for enhancing nanodiamond formation in electron cyclotron resonance plasma
J. Vac. Sci. Technol. A **24**, 1802 (2006); 10.1116/1.2221322

Effects of bias frequency on reactive ion etching lag in an electron cyclotron resonance plasma etching system
J. Vac. Sci. Technol. A **15**, 664 (1997); 10.1116/1.580702

Re-register for Table of Content Alerts

Create a profile.

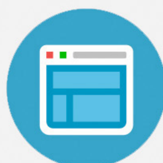

Sign up today!

Redistribution subject to AVS license or copyright; see http://scitation.aip.org/termsconditions. Download to IP: 140.113.38.11 On: Thu, 01 May 2014 02:35:56

Morphology control of silicon nanotips fabricated by electron cyclotron resonance plasma etching

C. H. Hsu, Y. F. Huang, and L. C. Chen
Center for Condensed Matter Sciences, National Taiwan University, Taipei 106, Taiwan

S. Chattopadhyay[a] and K. H. Chen
Institute of Atomic and Molecular Sciences, Academia Sinica, Taipei 106, Taiwan

H. C. Lo and C. F. Chen
Department of Materials Science and Engineering, National Chiao Tung University, Hsinchu 300, Taiwan

(Received 9 May 2005; accepted 12 December 2005; published 20 January 2006)

Formation of well-aligned silicon nanotips etched monolithically from a silicon substrate has been demonstrated. The effect of the process temperature on the physicochemical etching of silicon and subsequent fabrication of these nanotips has been investigated. 2.2-μm-long nanotips were formed at the process temperature of 250 °C and then decreased in length with increasing process temperature. Above 800 °C, the formation of the silicon nanotips was inhibited. Spectroscopic evidence attributes this fact to the efficient formation of silicon carbide thin film at higher process temperatures, instead of discontinuous nanomasks at lower process temperatures that prevent etching of the substrate. Another reason for this inhibited formation of nanotips is the reduced etching rate of the silicon by agents such as atomic H at higher process temperatures. © *2006 American Vacuum Society.* [DOI: 10.1116/1.2163894]

I. INTRODUCTION

Among the widely published nanotubes, nanorods, and nanowires there have also been several reports on one dimensional (1D) conical structures. Starting from metallic,[1] silicon,[2] and diamond[3] nanotips, a wide variety of conical, needlelike structures has been reported in recent years. These include silicon nanotip,[2] nanocone,[4] and nanoneedle,[5] carbon nanotips,[6] ZnO nanoneedle arrays,[7] AlN nanotips,[8] and so forth. The sharp apex angle and relatively high aspect ratio make the nanotips promising for many applications. The fascinating structures of 1D nanomaterials and their unique properties are opening up applications in nanodevices,[9] such as field-emission displays,[10] laser diodes,[11] scanning probe microscopy,[12] solar cells,[13] biosensors,[14] and so on.

In our previous work,[15] we have demonstrated a self-masked dry-etching technique for fabricating silicon (Si) nanotips in one step. These Si nanotips exhibited a low turn-on field during field-emission measurements and inherent Si process compatibility.[16] Such tips have also been used in solar cells,[17] imprint lithography,[18] and molecular sensing.[19,20] However, the control of tip morphology is crucial for such wide-ranging applications. This letter reports the influence of process temperature on the mechanism of a self-masked dry-etching technique of Si, giving rise to the nanotip morphology.

II. EXPERIMENT

The processes were carried out in an electron cyclotron resonance (ECR) plasma reactor using a gas mixture of silane (SiH_4), methane (CH_4), argon (Ar), and hydrogen (H_2) as dry-etching gases. The details of the process can be found elsewhere.[15,16] The starting substrates were boron (B)-doped *p*-type silicon (100) wafers with a resistivity of 1–10 Ω cm. In this study, a set of experiments were performed with various process temperatures ranging from 250 to 850 °C by keeping a constant flow rate ratio of $SiH_4/CH_4/Ar/H_2 = 0.2:2:5:8$, a total pressure of 5.8 mTorr, and a power of 1200 W. The morphology of the silicon nanotips has been imaged with a JEOL 6700 field-emission scanning electron microscope (SEM). The x-ray photoelectron spectroscopy (XPS) was carried out in a PHI 1600 system. The Fourier transform infrared (FTIR) spectra were obtained with a Bomem (Hartmann-Braun) MB series FTIR spectrometer in the reflection mode. The resolution of the spectrum was 4 cm^{-1}.

III. RESULTS AND DISCUSSION

Figure 1(a) shows a typical cross-sectional SEM image of a well-aligned Si nanotip array fabricated at 300 °C with a uniform distribution and a high density of $\sim 3\times 10^{10}/cm^2$. Figures 1(b)–1(d) show cross-sectional SEM images of nanotip arrays grown at 400, 600, and 800 °C, respectively. A typical high-resolution transmission electron microscopy (HRTEM) image of a Si nanotip indicates that all of these nanotips were capped at the apex with SiC nanomasks.[16] We observed that the length and density of the nanotips decreased with increasing process temperature. At process temperatures exceeding 800 °C, for example, 850 °C, there was hardly any nanotip visible. Instead a thick-film-like morphology was observed. Figure 2 shows a plot of the nanotip length as a function of the process temperature. From 2200 nm at a process temperature of 250 °C, the length of these nanotips decreased to less than 300 nm at a process

[a]Author to whom correspondence should be addressed; electronic mail: sur@diamond.iams.sinica.edu.tw

Redistribution subject to AVS license or copyright; see http://scitation.aip.org/termsconditions. Download to IP: 140.113.38.11 On: Thu, 01 May 2014 02:35:56

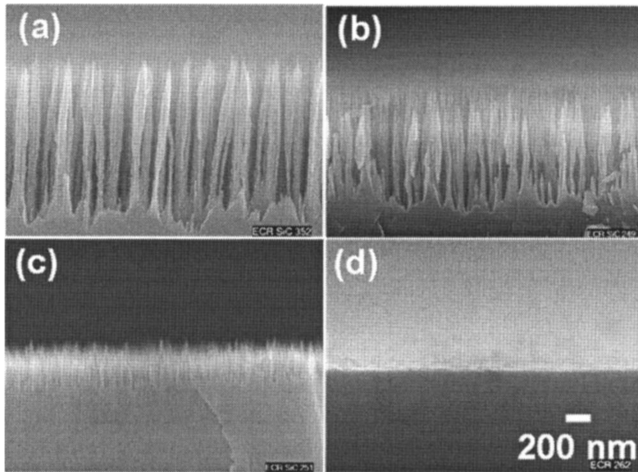

FIG. 1. Cross-sectional SEM images of Si nanotips prepared under process temperatures of (a) 300, (b) 400, (c) 600, and (d) 800 °C.

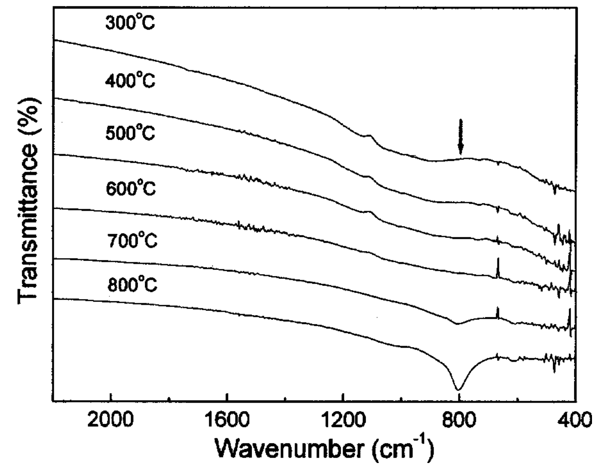

FIG. 3. FTIR spectra of the Si nanotips grown at different process temperatures (marked on each plot).

temperature of 600 °C and the formation of the nanotips were totally inhibited at temperatures above 800 °C.

FTIR spectroscopy was done to determine the bonding characterization of these nanotips as the process temperature was varied. As shown in the FTIR spectra (Fig. 3), the samples fabricated at low process temperatures did not exhibit any significant SiC signal until the process temperature exceeded 700 °C. A peak evolved at 800 cm^{-1} corresponding to the 3C–SiC (TO) mode.[21]

The weak peak located at approximately 600 cm^{-1} was due to the diffusion of excess carbon into the Si substrate during process.[22] XPS results corroborated the FTIR findings, qualitatively, by showing that the carbon content of the surface of the samples produced at 800 °C was much higher than those produced at 250 °C [Fig. 4(a)], whereas the silicon content at the surface was much lower for the sample fabricated at 800 °C [Fig. 4(b)].

At lower process temperatures, well-separated nanomasks of SiC may have existed on the Si substrate but remained undetectable due to minimal volume. Such SiC nanomasks, being harder to etch than silicon, however, still prevented uniform etching of the silicon substrate and gave rise to the nanotips. As the process temperature was increased, methane dissociation became more efficient in the vicinity of the silicon substrate and, instead of well-separated SiC nanomasks, a continuous layer of SiC or a carbon-rich SiC layer was formed. The formation of a SiC layer decreased the etching rate of silicon and finally inhibited further lengthening of nanotips. We estimated that the rate constants for dissocia-

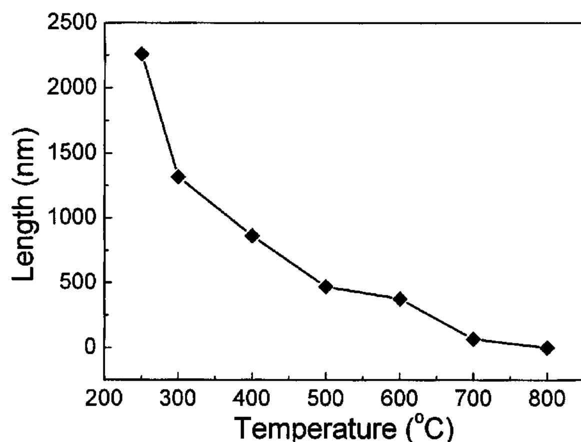

FIG. 2. Length of Si nanotips as a function of process temperature.

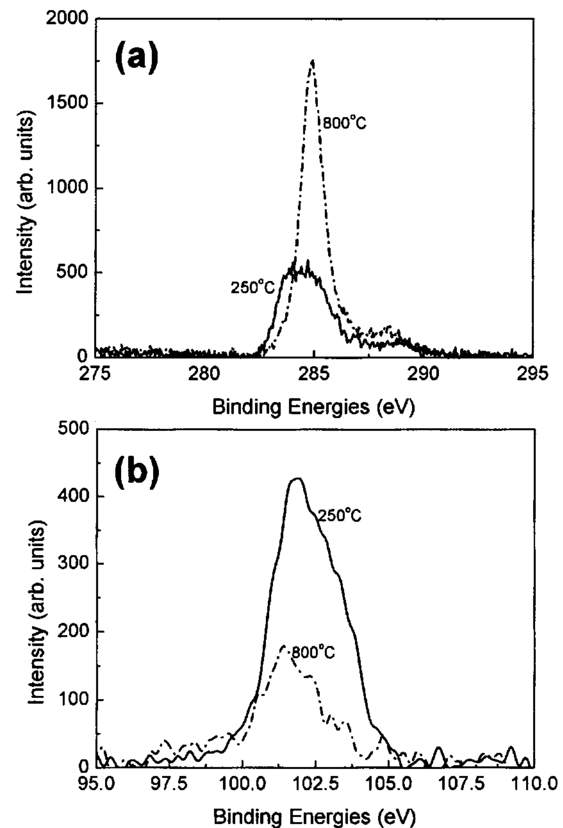

FIG. 4. (a) XPS C (1*s*) spectra of Si nanotip samples prepared at (—) 250 and (-----) 800 °C. (b) XPS Si (2*p*) spectra of Si nanotip samples prepared at (—) 250 and (-----) 800 °C.

Redistribution subject to AVS license or copyright; see http://scitation.aip.org/termsconditions. Download to IP: 140.113.38.11 On: Thu, 01 May 2014 02:35:56

tion of CH_4 were enhanced by two orders of magnitude from 1×10^9 at 250 °C to 1×10^{11} at 700 °C,[23] whereas the rate constants for the dissociation of SiH_4 increased from 1×10^{12} at 250 °C to 3×10^{12} at 700 °C. Moreover, at a process temperature of 700 °C, the dissociation rate constant for CH_4 is only one order smaller than that of SiH_4, which would predict an efficient pathway for the formation of SiC. In a plasma system the addition of SiH_4 can greatly enhance the deposition of SiC.[24] As SiH_4 can be dissociated into SiH_2 and SiH_3 radicals, CH_4 can similarly be dissociated to CH_3 or CH_2 radicals with the release of H through thermal dissociation or electron or Ar^* (excited Ar) impact dissociation in the ECR plasma. These radicals can react via a series of neutral-neutral reactions to result in radicals such as C_2H_2.[25] The silyl radicals can then react with C_2H_2 or CH_3 following a series of H abstraction to form SiC.[26]

For the surface-etching process, we apply the ion-assisted dry-etching theory. From our previous investigation, only physicochemical sputtering, instead of pure physical sputtering,[27] can contribute to a significant change in morphology when applied to different materials as substrates.[15] Therefore, ion-assisted chemical etching must occur through hydrogen atoms as etchant, for instance. Several other species are also involved in this etching, such as H, H^+, H_2^+, H_3^+, Ar^+, Ar_2^+, and ArH^+. It is known that ion bombardment can activate the surface, changing the surface reaction rates and mobility of reactive species. In the ECR plasma, the surface is bombarded by heavy ions causing a sputtering effect or molecular desorption from the Si substrate.

One can visualize the process as follows: First, H radicals are absorbed on the Si surface to form a layer of SiH. The formation of SiH_2, SiH_3, and subsequent gas-phase SiH_4 follows through reactions with H_3^+ and ArH^+ ions and reduction by H atoms. This mechanism becomes less probable due to the low sticking coefficients of these radicals on the Si substrates at higher temperatures, leading to a decrease of etching rate which is in accordance with our observation. Furthermore, Strass *et al.*[28] reported that there are two temperature regimes of Arrhenius dependence with different activation energies occurring in the hydrogen etching process. For temperatures above 300 °C the activation energy is −21 kcal/mol and that below 300 °C is only −1.7 kcal/mol. This leads to a decrease in etching rate when temperature is beyond 300 °C. Assuming the growth rate (R), in nm/h, of the nanotips to be proportional to the rate of any chemical reaction, including etching, taking place, we can plot the $\ln(R)$ as a function of inverse process temperature. This plot (Fig. 5) also reveals two activation energies of −134.2 and −19.9 kJ/mol above and below 600 °C, respectively. The difference in the activation energies in this case as against the values reported in Ref. 28 may have been caused by the fact that we are etching a partially masked (with SiC) silicon substrate, whereas Strass *et al.*[28] were etching silicon or silicon dioxide samples. In other words, the presence of both silane and methane will increase and decrease, respectively, the activation energies by forming the nanomasks and producing more etchants in the form of reactive H species.

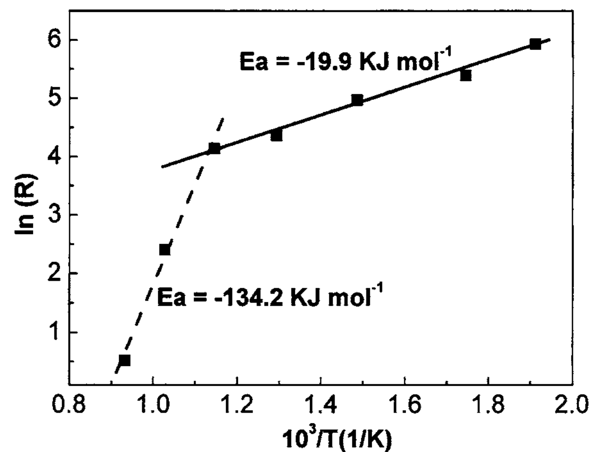

FIG. 5. Arrhenius plot of the etching rate as a function of inverse process temperature.

From Fig. 5, it is clear that our samples with process temperatures above 600 °C were much shorter than those produced below 600 °C. The experimental evidence of reduced nanotip length with increasing process temperature, along with the FTIR and XPS data put forward to support the formation of a continuous SiC film at higher process temperatures, clearly establishes the role of the SiC nanomasks in the formation of these Si nanotips and elucidates the dry-etching mechanism in Si.

IV. CONCLUSIONS

In summary, a temperature-controlled plasma etching of silicon substrates producing monolithic silicon nanotips has been described. The silicon nanotip originates from the nonuniform etching of the silicon substrate protected by SiC nanomasks in the reactive microwave plasma. The length of the Si nanotips decreased with increasing process temperature, and beyond 800 °C, the nanotip formation was inhibited. The observed length reduction and ultimate extinction of the nanotips with increasing process temperature are due to the growth of a continuous SiC film at high temperatures preventing effective etching. On the other hand, a low sticking coefficient of the hydrogen-related species reduced the effective chemical etching rate at higher process temperatures.

ACKNOWLEDGMENTS

The work was carried out with financial assistance from National Science Council, Ministry of Education, Taiwan, Air Force Office of Scientific Research, USA, and Asian Office of Aerospace Research and Development. One of the authors (S.C.) would like to acknowledge a fellowship from the Institute of Atomic and Molecular Science, Academia Sinica, Taiwan.

This paper was presented at the First International Workshop on One-Dimensional Materials, January 10–14, 2005, National Taiwan University, Taipei, Taiwan.

Redistribution subject to AVS license or copyright; see http://scitation.aip.org/termsconditions. Download to IP: 140.113.38.11 On: Thu, 01 May 2014 02:35:56

[1]C. H. Oon, J. T. L. Thong, Y. Lei, W. Lei, and W. K. Chim, Appl. Phys. Lett. **81**, 3037 (2002).
[2]M. H. Yun, V. A. Burrows, and M. N. Kozicki, J. Vac. Sci. Technol. B **16**, 2844 (1998).
[3]C. L. Tsai, C. F. Chen, and C. L. Lin, J. Appl. Phys. **90**, 4847 (2001).
[4]N. G. Shang, F. Y. Meng, F. C. K. Au, Q. Li, C. S. Lee, I. Bello, and S. T. Lee, Adv. Mater. (Weinheim, Ger.) **14**, 1308 (2002).
[5]M. Kanechika, N. Sugimoto, and Y. Mitsushima, J. Vac. Sci. Technol. B **20**, 1843 (2002).
[6]C. L. Tsai, C. F. Chen, and C. L. Lin, Appl. Phys. Lett. **80**, 1821 (2002).
[7]W. I. Park, G. C. Yi, M. Kim, and S. J. Pennycook, Adv. Mater. (Weinheim, Ger.) **14**, 1841 (2002).
[8]S. C. Shi, C. F. Chen, S. Chattopadhyay, Z. H. Lan, K. H. Chen, and L. C. Chen, Adv. Funct. Mater. **15**, 781 (2005).
[9]Z. L. Wang, Adv. Mater. (Weinheim, Ger.) **12**, 1295 (2000).
[10]W. B. Chou, D. S. Chung, J. H. Kang, H. Y. Kim, Y. W. Jin, I. T. Han, Y. H. Lee, J. E. Jung, N. S. Lee, G. S. Park, and J. M. Kim, Appl. Phys. Lett. **75**, 3129 (1999).
[11]M. H. Huang, S. Mao, H. Feick, H. Q. Yan, Y. Y. Wu, H. Kind, E. Weber, R. Russo, and P. Yang, Science **292**, 1897 (2001).
[12]H. Dai, J. H. Hafner, A. G. Rinzler, A. G. Colbert, and R. E. Smalley, Nature (London) **384**, 147 (1996).
[13]W. U. Huynh, J. J. Dittmer, and A. P. Alivisatos, Science **295**, 2425 (2002).
[14]J. N. Wohlstadter, J. L. Wilbur, G. B. Sigal, H. A. Biebuyck, M. A. Billadeau, L. Dong, A. B. Fischer, S. R. Gudibande, S. H. Jameison, J. H. Kenten, J. Leginus, J. K. Leland, R. J. Massey, and S. J. Wohlstadter, Adv. Mater. (Weinheim, Ger.) **15**, 1184 (2003).
[15]C. H. Hsu, H. C. Lo, C. F. Chen, C. T. Wu, J. S. Hwang, D. Das, J. Tsai, L. C. Chen, and K. H. Chen, Nano Lett. **4**, 471 (2004).
[16]H. C. Lo, D. Das, J. S. Hwang, K. H. Chen, C. H. Hsu, C. F. Chen, and L. C. Chen, Appl. Phys. Lett. **83**, 1420 (2003).
[17]H. Yoshida, Y. Terada, H. Miyake, and K. Hiramatsu, Jpn. J. Appl. Phys., Part 2 **41**, L1134 (2002).
[18]S. Y. Chou, P. R. Krauss, and P. J. Renstrom, Appl. Phys. Lett. **67**, 3114 (1995).
[19]S. Chattopadhyay, H. C. Lo, C. H. Hsu, L. C. Chen, and K. H. Chen, Chem. Mater. **17**, 553 (2005).
[20]S. Chattopadhyay, S. C. Shi, C. F. Chen, L. C. Chen, and K. H. Chen, J. Am. Chem. Soc. **127**, 2820 (2005).
[21]S. Liedtke, K. Jahn, F. Finger, and W. Fuhs, J. Non-Cryst. Solids **77/78**, 849 (1985).
[22]Y. Sun, T. Miyasato, and N. Sonoda, J. Appl. Phys. **84**, 6451 (1998).
[23]M. J. Rabinowitz, J. W. Sutherland, P. M. Patterson, and R. B. Klemm, J. Phys. Chem. **95**, 674 (1991).
[24]I. Solomon, M. P. Schmidt, and H. Tran-Quoa, Phys. Rev. B **38**, 9895 (1988).
[25]W. L. Hsu, J. Appl. Phys. **72**, 3102 (1992).
[26]W. H. Lee, J. C. Lin, C. Lee, H. C. Cheng, and T. R. Yew, Diamond Relat. Mater. **10**, 2075 (2001).
[27]P. Cuerno and A. L. Barabasi, Phys. Rev. Lett. **74**, 4746 (1995).
[28]A. Strass, W. Hansch, P. Bieringer, A. Neubecker, F. Kaesen, A. Fischer, and I. Eisele, Surf. Coat. Technol. **97**, 158 (1997).

Redistribution subject to AVS license or copyright; see http://scitation.aip.org/termsconditions. Download to IP: 140.113.38.11 On: Thu, 01 May 2014 02:35:56